Chapter 4

Large scale shell model calculations for $^{61-66}$Fe isotopes

4.1 Introduction

The neutron rich nuclei in the *fp* shell region are at the focus of attention of the nuclear physics community at present. Unstable nuclei in this region exhibit many new phenomenon such as appearance of new magic numbers and disappearance of well established ones, softening of core at N=28, interplay of collective and single particle properties *etc*. Neutron rich *fp* shell nuclei are also of special interest in astrophysics such as the electron capture rate in supernovae explosion. A large number of neutron rich nuclei can be populated by means of binary reactions such as multinucleon transfer and deep inelastic collisions with a stable beam. Such reactions combined with modern γ detector arrays have increased substantially the available data on nuclei far from stability. Experimental data on the excited states of neutron rich unstable isotopes of Ca, Ti and Cr has been made available in recent past [NNDC]. Recently at Legnaro National Laboratories neutron rich Fe isotopes from A=61-66 were populated through multineutron transfer reaction by bombarding a ^{238}U target with 400MeV ^{64}Ni beam [Lur07]. The identification of γ-rays belonging to each nucleus was carried out with high precision by coupling the clover detector of Euroball (CLARA) to PRISMA magnetic spectrometer. This experiment has provided data on level structure of neutron rich Fe isotopes from A=61 to 66.

The Nuclear shell model is one of the most powerful tools for giving a quantitative interpretation to the experimental data. The two main ingredients of any shell model calculations are the N-N interaction and the configuration space for valence particles. In principle one can either perform shell model calculations with realistic N-N interaction in unlimited configuration space or with renormalized

effective interaction in a limited configuration space. Various methods have been adopted in the literature to obtain effective interaction from realistic N-N interaction. One of the methods is to modify the matrix elements of the microscopic interaction by carrying an empirical fit to a sufficiently large body of experimental data. Using this approach Honma *et al.* [Hon04a] have derived an effective interaction, GXPF1, from Bonn-C potential for *fp* shell and have used it in the shell model calculations in full *fp* configuration to obtain the systematics of neutron rich isotopes of Ca, Cr and Ti. Their analysis showed significant deviation from the experimental data towards the end of *fp* shell. As GXPF1 was derived by fitting the experimental data of stable isotopes, some modifications in the interaction were required for its use for predicting the structure of unstable nuclei in the *fp* shell. In view of this the interaction was modified by changing five matrix elements (three of pairing interaction and two of quadrupole-quadrupole interaction). This modified interaction, known as GXPF1A [Hon04b], improved the agreement with experimental data for unstable isotopes in *fp* region. Lunardi *et al.* [Lur07] have interpreted the results of their experiments on $^{61-66}$Fe isotopes by performing large scale shell model calculations with an effective interaction 'fpg' described in Ref [Sor02]. In their calculation an inert core of ^{48}Ca is considered and the valence space chosen is the whole *fp* shell for the protons and the $p_{3/2}$ $f_{5/2}$ $p_{1/2}$ and $g_{9/2}$ orbitals for the neutrons. In order to reduce the dimensions of the matrices involved a truncation was put on the number of particles allowed to be excited: a maximum of x protons were allowed to be excited from the $f_{7/2}$ to the rest of the *fp* shell and (n-x) neutrons from three *fp* orbitals to $g_{9/2}$ orbital where n=5.

In the present work we have performed large scale shell model calculations on neutron rich $^{62-66}$Fe isotopes with GXPF1A interaction without any truncation. The calculations have been carried out in valence space of full *fp* shell consisting of $0f_{7/2}$ $1p_{3/2}$ $0f_{5/2}$ $1p_{1/2}$ orbitals and treating ^{40}Ca as the inert core. No restriction has been put on the number of particles which can be excited to higher level. The aim of this paper is to test the suitability of GXPF1A interaction towards the end of *fp* shell. Also by comparing the results of present work with that of Ref [Lur07] one can get some insight on the role of $g_{9/2}$ orbit in explaining the data.

4.2 Details of Calculation

4.2.1 Configuration space

Large scale shell model calculations have been performed for neutron rich Fe isotopes with A=61, 62, 63, 64, 65, 66 treating ^{40}Ca as inert core. The configuration space

for valence particles is taken as full *fp* shell which is made up of all Pauli allowed combinations of valence particles in the $0f_{7/2}$, $1p_{3/2}$, $0f_{5/2}$ and $1p_{1/2}$ orbitals for both the protons and neutrons. The single particle energies for model space $0f_{7/2}$, $1p_{3/2}$, $1p_{1/2}$, $0f_{5/2}$ are -8.6240, -5.6793, -4.1370 and -1.3829 MeV respectively.

4.2.2 Effective Interaction

The calculations have been performed with a newly derived effective interaction GXPF1A obtained from a fit to the experimental data of unstable nuclei in the *pf* shell. Honma *et al.* [Hon04a] initially derived an effective interaction, GXPF1, starting from Bonn-C potential by modifying 70 well determined combinations of 4 single particle energies and 195 two body matrix elements by iterative fitting calculations to about 699 experimental energy data out of 87 stable nuclei. These authors have tested the GXPF1 interaction for the shell model calculations in the full *fp* shell extensively [Hon04b] from various viewpoints such as binding energies, electromagnetic moments and transitions, and excitation spectra in the wide range of *fp* shell nuclei. They observed that the deviation of the shell model prediction from available experimental data appeared to be sizable in binding energies of $N \geq 35$ nuclei and in magnetic moments of $Z \geq 32$ even-even nuclei. For the unstable nuclei, whereas the experimental data on Ca and Cr isotopes were well explained with GXPF1A, the experimental value of the first excited 2^+ state of ^{56}Ti was lower than the predicted value by about 0.4 MeV requiring modification of the interaction. The interaction was modified by these authors by changing 5 two body matrix elements in the *fp* shell: 3 pairing interaction matrix elements were made slightly weaker and two quadrupole-quadrupole matrix elements were made slightly stronger [Hon04b]. The modified interaction, referred to as GXPF1A, gave improved description simultaneously for all these three isotope chains and is reliable for use in shell model calculations to explain the data on unstable nuclei.

4.2.3 Computer code

The calculations have been performed at the SGI-cluster computer at GANIL with the code `ANTOINE` [Cau89] [Cau99]. In this code the problem of giant matrices is solved by splitting the valence space into two parts, one for the proton and another for the neutron. The states of the basis are written as the product of two Slater determinants (SD), one for the protons and another for the neutrons: $\mid I\rangle = \mid i, \alpha\rangle$. (Here capital letter refers to full space and lower case letters refer to subspaces of proton and neutron). The Slater determinants i and α can be classified by their M

values, M_1 and M_2. The total M being fixed, the SD of the two subspaces will be associated only if $M_1 + M_2 = M$. Dimensions of the matrices involved for $^{62-66}$Fe in m-scheme are given in Table 4.1 for different J states.

Table 4.1: Dimensions of matrices involved for $^{62-66}$Fe in the m scheme for *fp* shell .

J^π	^{62}Fe	^{64}Fe	^{66}Fe
0^+	14625240	634744	3952
2^+	14358186	620567	3815
4^+	13586777	580340	3496
6^+	12386760	518387	2984
8^+	10876432	442325	2406

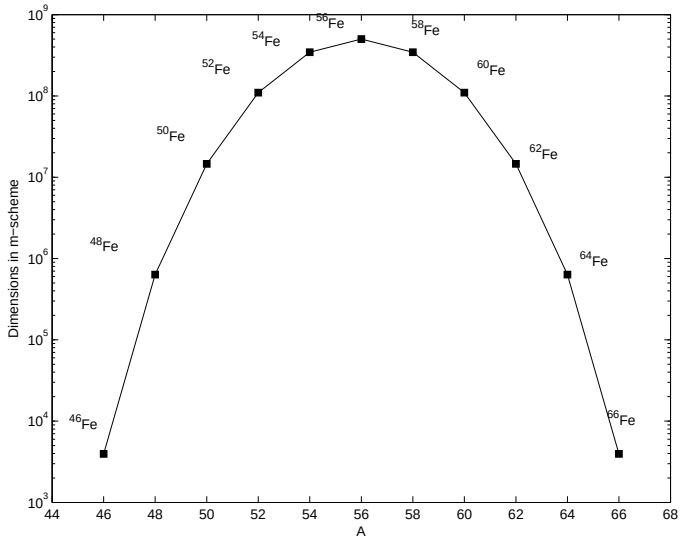

Figure 4.1: Dimensions of the matrices for 0^+ state in the m-scheme as a function of A.

The dimensionality of the matrices is maximum at midshell and decreases very fast towards the beginning and at the end of the shell as shown in Fig. 4.1. The computing time for ^{62}Fe was three days compared to two hours for ^{66}Fe.

4.3 Results and discussions for even-even $^{62-66}$Fe isotopes

4.3.1 Excitation energies and comparison with the data

The calculated energy levels obtained with GXPF1A interaction for even Fe isotopes are shown in Fig. 4.2-4.4 and compared with the experimental data and also with the results obtained with '*fpg*' interaction in a truncated configuration space. It is observed that large scale shell model calculation with GXPF1A interaction in full *fp* space gives very good agreement with the experimental data for ^{62}Fe. For 2^+ , 4^+ and 6^+ states of ^{62}Fe the discrepancies with experimental data are 70, 5 and 138 KeV respectively whereas with '*fpg*' interaction the corresponding values are 6, 219 and 494 KeV. But the discrepancy with the experimental data increases as we go towards N=40. The '*fpg*' interaction with truncation on the number of particles getting excited gives better result. This shows the importance of $g_{9/2}$ orbital in explaining the data for A=66. This can be understood in terms of decrease in the energy gap between *fp* shell and $1g_{9/2}$ orbital in going towards N=40 and can be attributed to the proton neutron monopole tensor interaction [Hon04a]. Variation of the first 2^+ excited state energy levels E(2^+) with neutron number is shown in Fig. 4.5. Thus the recent data on ^{62}Fe can be explained very well in the frame work of large scale shell model calculations with GXPF1A interaction in full *fp* space with no truncation, without including $0g_{9/2}$ orbital. The fit is reasonably satisfactory for ^{64}Fe, but agreement with the experimental data on ^{66}Fe is not good.

4.3.2 Wave functions

The wave functions for $^{62-66}$Fe isotopes are shown in Table 4.2. The most dominant contribution in the ground state of ^{62}Fe is $(0f_{7/2})^8$, $(1p_{3/2})^4$, $(1p_{1/2})^0$, $(0f_{5/2})^4$ whereas that of ^{64}Fe is $(0f_{7/2})^8$, $(1p_{3/2})^4$, $(1p_{1/2})^2$, $(0f_{5/2})^4$ indicating change in the ordering of $1p_{1/2}$ and $0f_{5/2}$ levels.

4.3.3 Electromagnetic properties

The calculated B(E2) values for $2_1^+ \rightarrow 0_{gs}^+$ transition are shown in Table 4.3 for $^{62-66}$Fe, using standard effective charges e_π=0.5 and e_ν=1.5 respectively [Boh69] [Bro05]. A free neutron does not have any charge but nucleons in the nucleus can polarize the core by interacting with nucleons of the core. This is reflected by giving the neutron an effective charge. The B(E2) values obtained in the present

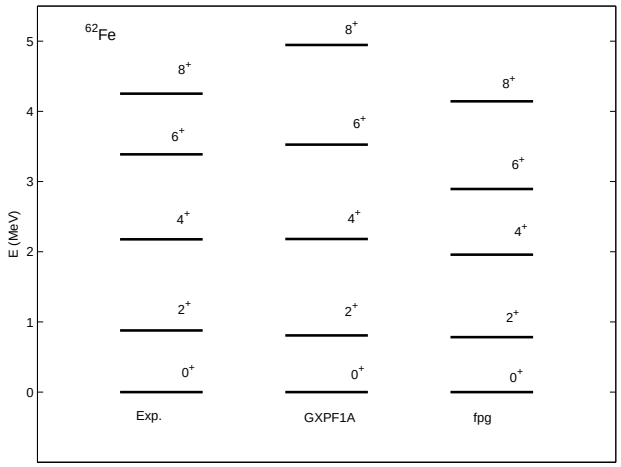

Figure 4.2: Calculated energy levels of ^{62}Fe with GXPF1A interaction compared with the experimental data and the previous theoretical work using '*fpg*' interaction with the truncation from Ref. [Lur07].

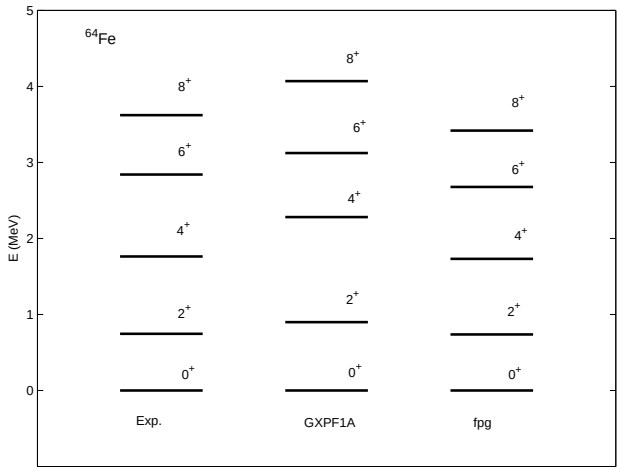

Figure 4.3: Same as Fig 4.2 for ^{64}Fe.

calculation are plotted in Fig. 4.6 as a function of neutron number along with the available experimental data for lighter Fe isotopes in the same figure.

The results obtained with GXPF1A show a large increase in the value of $E_{ex}(2^+)$ and decrease in $B(E;2_1^+ \rightarrow 0_{gs}^+)$ at N=40 - a feature typical of shell closure at N=40. Similar pattern is obtained for N=28. In contrast to this, the experimental value of the first 2^+ exited state decreases with increasing number of neutrons when approaching N=40. The drop in the excitation energy is a signature for increasing

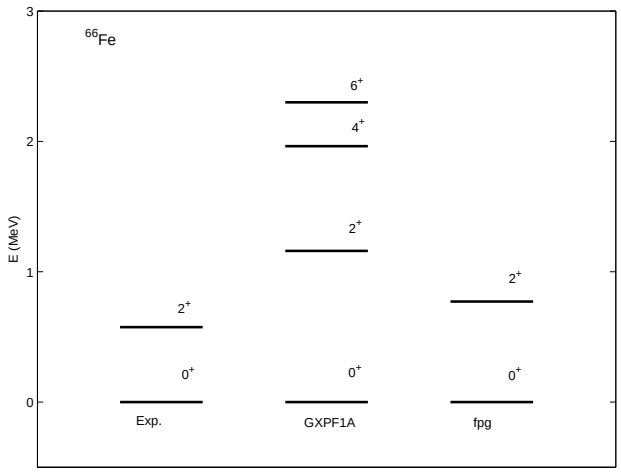

Figure 4.4: Same as Fig 4.2 for ^{66}Fe.

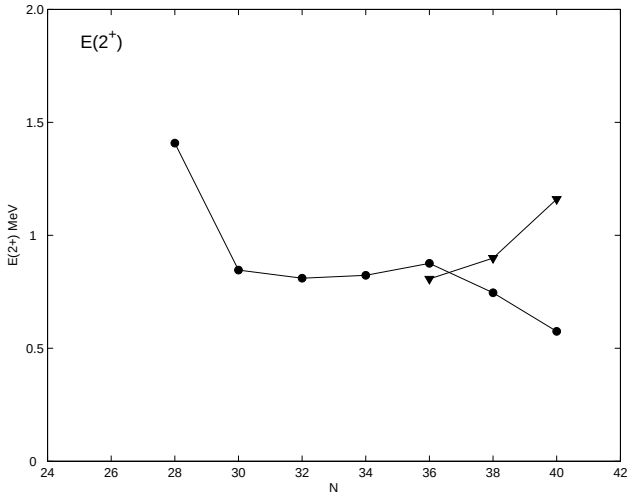

Figure 4.5: First 2^+ energy levels as a function of neutron number N. Experimental data are shown by filled circle and results from the present work by filled triangle.

collectivity. This feature could not be explained with GXPF1A and the calculated excitation energy of 2^+ state is predicted too high. This indicates that the considered valence space is not large enough to account for increase of collectivity at N=40. The results obtained with '*fpg*' interaction are better. This shows the importance of $g_{9/2}$ orbital in explaining the data for A=66.

Table 4.2: Main configurations in the wave functions of the ground state and the first exited state for $^{62-66}$Fe calculated with GXPF1A interaction.

Nuclei	J^π	Wave function		Probability
		Neutron	Proton	
^{62}Fe	0^+_{gs}	$(0f_{7/2})^8,(1p_{3/2})^4,(1p_{1/2})^0,(0f_{5/2})^4$	$(0f_{7/2})^6$	34.4
	2^+_1	$(0f_{7/2})^8,(1p_{3/2})^4,(1p_{1/2})^0,(0f_{5/2})^4$	$(0f_{7/2})^6$	28.8
^{64}Fe	0^+_{gs}	$(0f_{7/2})^8,(1p_{3/2})^4,(1p_{1/2})^2,(0f_{5/2})^4$	$(0f_{7/2})^6$	73.3
	2^+_1	$(0f_{7/2})^8,(1p_{3/2})^4,(1p_{1/2})^2,(0f_{5/2})^4$	$(0f_{7/2})^6$	71.5
^{66}Fe	0^+_{gs}	$(0f_{7/2})^8,(1p_{3/2})^4,(1p_{1/2})^2,(0f_{5/2})^6$	$(0f_{7/2})^6$	96.6
	2^+_1	$(0f_{7/2})^8,(1p_{3/2})^4,(1p_{1/2})^2,(0f_{5/2})^6$	$(0f_{7/2})^6$	95.5

Table 4.3: Excitation energies, quadrupole moments and B(E2) for $^{62-66}$Fe isotopes.

	^{62}Fe	^{64}Fe	^{66}Fe
$E(2^+)$(MeV)	0.807	0.899	1.160
$E(4^+)$(MeV)	2.181	2.281	1.963
$Q(2^+)(efm^2)$	-26	-19	-17
B(E2)(W.u.)	14.8	10.1	5.4

4.4 Results and discussions for even-odd $^{61-65}$Fe isotopes

4.5 Results and discussions

The results of our calculation obtained with GXPF1A interaction for $^{61-65}$Fe isotopes are shown in Fig. 4.7-4.9 and compared with the experimental data and also with the results of Lurandi *et al*. obtained with *fpg* interaction in a truncated configuration space [Lur07]. In the case of ^{61}Fe the calculated energy difference between$1/2^-$ and $3/2^-$ is only of the order of 86 KeV. If this difference being less than 100 KeV neglected, the ordering of the levels is correctly reproduced. For *fpg* interaction also $1/2^-$ level lies 36 KeV below $3/2^-$ level and has been suppressed in the figure (Lurandi *et al*. private communication). The calculated $7/2^-$ state is at 988 KeV above the ground state compared to the experimental value of 959 KeV. In the case of ^{63}Fe measured ground state spin is $5/2^-$ and the first excited $3/2^-$ state lies above 356 KeV. GXPF1A interaction predicts ground state spin as $3/2^-$ after suppresing $1/2^-$. The same is true for *fpg* interaction. The first excited state is at 298 KeV with spin $5/2^-$ and next state is at 1152 KeV with spin $5/2^-$. The $\epsilon_{5/2^-} \sim \epsilon_{3/2^-}$ energy difference is 298 KeV for GXPF1A interaction and 192 KeV for

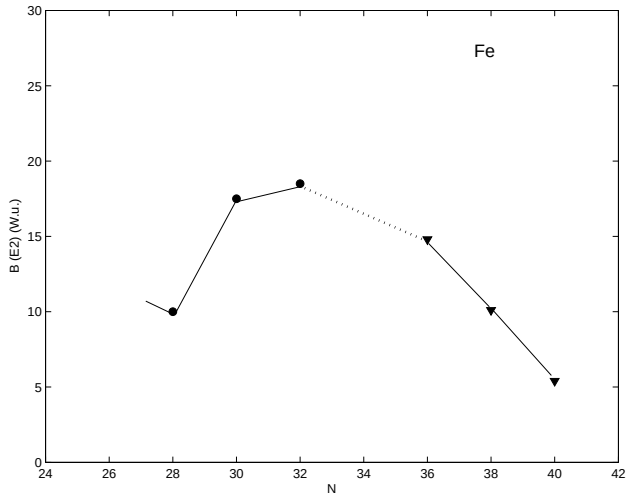

Figure 4.6: B(E2;$2_1^+ \rightarrow 0_{gs}^+$) for $^{54-58}$Fe from Ref [Hon04a] by filled circle and results from the present work by filled triangle for $^{62-66}$Fe .

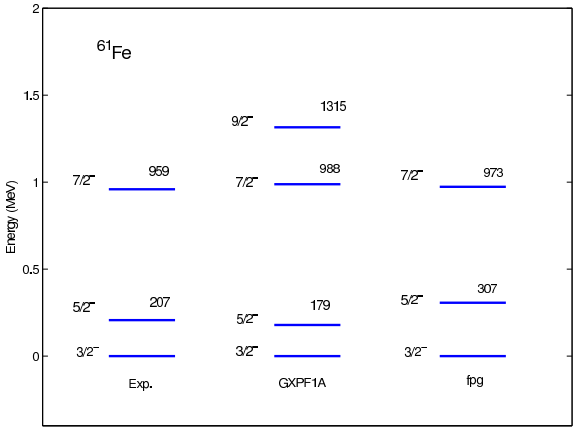

Figure 4.7: Calculated energy levels of ^{61}Fe with GXPF1A interaction compared with the experimental data and the previous theoretical work using *fpg* interaction with truncation from Ref. [Lur07].

fpg interaction compared to the experimental value of 356 KeV. For ^{65}Fe only one excited level at 364 KeV has been measured with unassigned spin. This compares favourably with the calculated $1/2^-$ state at 370 KeV.

The most dominant contribution in the wave function for the ground state and the first excited state for odd-even $^{61-65}$Fe isotopes are given in Table 4.4. Neutron occupation numbers of the $0f_{5/2}$ and $1p_{1/2}$ levels for the ground state and first excited states are shown in Fig.4.10 as a function of neutron number. In going from ^{61}Fe

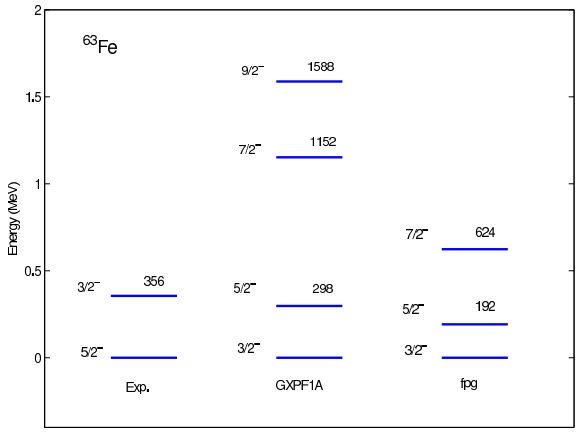

Figure 4.8: Calculated energy levels of ^{63}Fe with GXPF1A interaction compared with the experimental data and the previous theoretical work using *fpg* interaction with truncation from Ref. [Lur07].

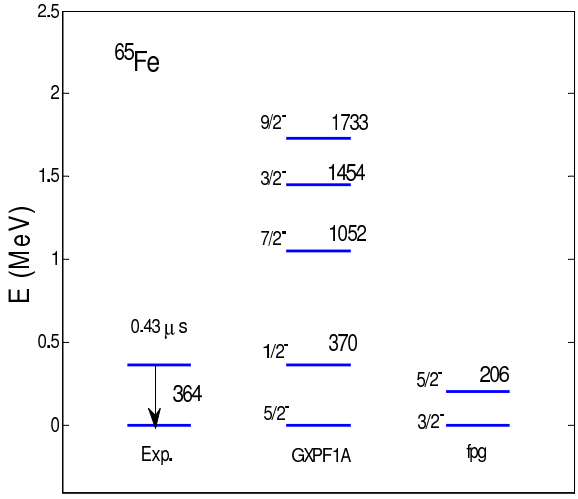

Figure 4.9: Calculated energy levels of ^{65}Fe with GXPF1A interaction compared with the experimental data and the previous theoretical work using *fpg* interaction with truncation from Ref. [Lur07].

to ^{63}Fe for the ground state the occupancy of $1p_{1/2}$ level remains constant whereas that of $0f_{5/2}$ increases from 2 to 4. For the first excited state the occupancy of $1p_{1/2}$ level rises from 0 to 1 and that of $0f_{5/2}$ level from 3 to 4. In the most dominant configuration for the ground state in ^{61}Fe, $1p_{1/2}$ level is half filled and $0f_{5/2}$ level is relatively more important. In the first excited state of ^{61}Fe, $1p_{1/2}$ state is unoccupied. In ^{63}Fe, $1p_{1/2}$ state is only partially occupied. In the case of ^{63}Fe the ground state spin and the correct ordering of the energy levels is not predicted with GXPF1A

Table 4.4: Main configurations in the wave functions of the ground state and the first exited state for $^{61-65}$Fe calculated with GXPF1A interaction.

Nuclei	J^π	Wave function		Probability
		Neutron	Proton	
^{61}Fe	$\frac{3}{2}^-$	$(0f_{7/2})^8,(1p_{3/2})^4,(1p_{1/2})^0,(0f_{5/2})^3$	$(0f_{7/2})^6$	23.7
^{63}Fe	$\frac{3}{2}^-$	$(0f_{7/2})^8,(1p_{3/2})^4,(1p_{1/2})^1,(0f_{5/2})^4$	$(0f_{7/2})^6$	58.5
^{65}Fe	$\frac{5}{2}^-$	$(0f_{7/2})^8,(1p_{3/2})^4,(1p_{1/2})^2,(0f_{5/2})^5$	$(0f_{7/2})^6$	90.0

interaction as also was the case with *fpg* interaction. The wave function structure shown in Table 4.4 indicates preferred filling of $0f_{5/2}$ levels over the $1p_{1/2}$ level in almost all the cases. This indicates that the single particle energy levels get renormalized due to the monopole effect. These attractive and repulsive interactions affect cooperatively the single particle energies and may change the ordering of levels.

In the case of ^{63}Fe the ground state spin and the correct ordering of the energy levels is not predicted with GXPF1A interaction as also was the case with *fpg* interaction. The wave function structure shown in table indicates preferred filling of $0f_{5/2}$ levels over the $1p_{1/2}$ level. This indicates that the single-particle energy levels get renormalized due to the monopole effect. These attractive and repulsive interactions affect cooperatively the single-particle energies and may change the ordering of levels.

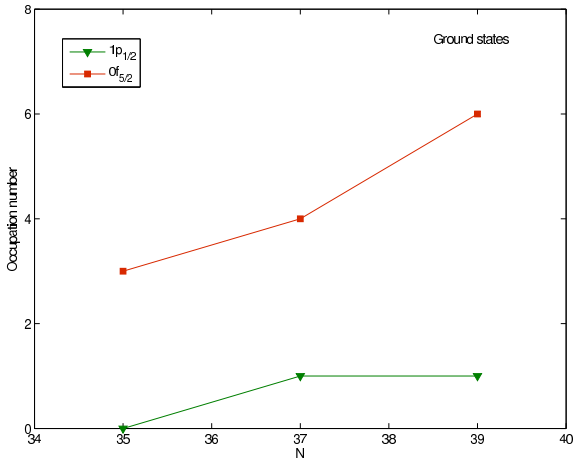

Figure 4.10: Neutron occupation number of the *fp* shell orbits for ground states in even-odd $^{61-65}$Fe isotopes.

4.6 Conclusions

In the present work large scale shell model calculations have been performed for neutron rich even isotopes of Fe with A=61, 62, 63, 64, 65, 66 in full *fp* space without truncation with recently derived GXPF1A interaction suitable for use in *fp* shell for the unstable nuclei. The experimental data is very well reproduced for ^{62}Fe and the agreement is better than the earlier calculations carried out in *fpg* configuration space with truncation imposed on the maximum number of particles getting excited to higher levels. This indicates that full *fp* space is sufficient for ^{62}Fe nucleus. The agreement with the experimental data is reasonably satisfactory for ^{64}Fe and is almost same as those obtained with *fpg* configuration space. The agreement gets worse for ^{66}Fe showing the inadequacy of the chosen configuration space. The results of our calculations for even-odd Fe isotopes show that the levels are well reproduced with GXPF1A interaction and for lower levels the agreement is better than that with *fpg* interaction. This indicates that full *fp* space is sufficient for explaining the negative parity states of ^{61}Fe and inclusion of $0g_{9/2}$ is not important. The ground state spin and the ordering of the two experimentally known levels of ^{63}Fe has not been correctly reproduced for both the interactions. The ground state spin of ^{63}Fe can be explained as arising from the $\nu(0f_{5/2})\otimes 0^{+}(^{62}\mathrm{Fe})$ configuration. The structure of wave functions for these isotopes suggest that single particle energy levels get modified due to monopole interaction which plays a decisive role in filling the levels.